Journal of Ceramic Processing Research. Vol. 14, No. 4, pp. 453~458 (2013)

J O U R N A L O F
Ceramic Processing Research

One-step fabrication and photoluminescence of alumina-sheathed GaN nanowires

Dong Sub Kwak[a], Yong Jung Kwon[a], Hong Yeon Cho[a], Chongmu Lee[b], and Hyoun Woo Kim[a,*]
[a]*Division of Materials Science and Engineering, Hanyang University, Seoul 133-791, Korea*
[b]*Division of Materials Science and Engineering, Inha University, Incheon 402-751, Korea*

Gallium nitride (GaN)/alumina (Al_2O_3) core-shell structures were successfully synthesized by a simple and one-step thermal evaporation method. We characterized their morphology, microstructures, and optical properties by SEM, TEM, EDX, and photoluminescence (PL). The core-shell structures were comprised of a core of single crystalline, GaN nanowires surrounded by a shell of Al_2O_3 tubular structures. We proposed a base-growth process as the dominant mechanism for the growth of the core/shell nanowires. We have discussed the possible reason for the preferential formation of the Al_2O_3 shells on the outside of the core-shell structures. In regard to the core/shell structures, an emission peak of 3.3 eV was observed in the room-temperature PL measurements in addition to the GaN-associated peaks, and was attributed to the Al_2O_3 shell.

Key words: GaN, Nanowires, Alumina, Photoluminescence, Growth mechanism.

Introduction

Hexagonal gallium nitride (GaN) has a large bandgap, high melting point, saturation drift velocity, breakdown field, and chemical inertness. Accordingly, it is most attractive material for the fabrication of high temperature and high power optoelectronic devices, blue and ultraviolet light-emitting diodes and laser diodes [1, 2]. With various nanostructures exhibiting specific physical and chemical properties [3-28], the GaN nanowires has a higher surface-to-volume ratio, resulting in a higher-sensitivity for a GaN-based gas sensor and the successful application of such nanowires in future field emission displays [29, 30]. In fabricating GaN nanowires [31-33], their finite size confines the electron wave functions and quantizes the energy levels, significantly modifying the transport and optical properties [34].

In recent years, radial heterostructured nanowires have been developed to enhance the functionality of nanowires and to protect against contamination [35]. In general, insulating shells offer a lot of advantages [36-38], including chemical stability, insulating characteristics, and protection from contamination, mechanical and radiation damage. Such shells can be used to prevent strong noise in nanocircuits and they protect against unnecessary charge injection, and partially screen external fields [6, 39]. Also, the coating on GaN nanowires can improve the electron emission uniformity and capability [40].

In particular, an Al_2O_3 shell has been found to be effective in enhancing physical and chemical properties, for a variety of academic and industrial applications. Owing to the importance of such shells, numerous researchers have fabricated low-dimensional nanomaterials surrounded by an Al_2O_3 shell. For electronic applications, the passivation by a thin Al_2O_3 shell has been found to effectively remove dispersion and has improved transport properties in the channel of InAlN/GaN high-electron mobility transistors [41]. Since such a shell can play a role as a gate dielectric in coaxial field effect transistors (FETs) [42], it is crucial to study the characteristics of the Al_2O_3 shell layer on GaN nanowires. A GaN metal-organic FET (MOSFET) based on an atomic layer deposition (ALD) Al_2O_3 coating as a gate dielectric has been shown to have excellent dc output as well as transfer characteristics [43]. In Al_2O_3-coated In_2O_3 nanostructures, the Al_2O_3 shell remarkably decreased the effective work function and improved the field emission capabilities [44]. For optical applications, in ZnO/Al_2O_3 core-shell nanorod arrays, the Al_2O_3 shell generates a flat-band effect near the ZnO surface, resulting in a stronger overlap of the wave functions of carriers in the ZnO core and further enhancing the near-band-edge (NBE) emission [45]. In addition, the photoluminescence (PL) of the GaQ(3)-Al_2O_3 core-shell nanowires was not degraded in air and water vapor and was only degraded in oxygen, but to a lesser degree than uncalted nanowires [46]. Therefore, the Al_2O_3 shell was found to be effective in protecting the PL of nanowires. Peapodlike SiO_x/Al_2O_3 heterostructures showed a stable and strong blue emission [47].

For magnetic applications, the Al_2O_3 shell in Ni/Al_2O_3 core-shell nanowires has been used to prevent oxidation and thus to maintain magnetic memory capabilities [48]. The Fe_3O_4/Al_2O_3 core-shell microspheres not only have

*Corresponding author:
Tel : +82-2-2220-0382
Fax: +82-2-2220-0389
E-mail: hyounwoo@hanyang.ac.kr

an Al_2O_3 shell, giving them a high-trapping capacity for phosphopeptides, but also have a magnetic property that enables easy isolation by positioning of an external magnetic field [49]. In the $FeNi_3/Al_2O_3$ core-shell nanocomposites, the Al_2O_3 insulating shell improves the soft magnetic properties of the $FeNi_3$ alloy [50]. Besides, the Fe_3O_4/Al_2O_3 core-shell nanoparticles can be used to obtain the highly specific capture of heme proteins for direct electrochemistry [51]. In ZnO/Al_2O_3 core-shell nanowire dye-sensitized solar cells, the Al_2O_3 shell acts as an insulating barrier to improve cell open-circuit voltage (V_{OC}) [52].

In spite of their importance, GaN/Al_2O_3 core-shell nanowires and their synthesis methods have been only rarely studied. Kang et Al. reported on the fabrication of Al_2O_3-coated GaN nanowires by means of employing the ALD method [53]. In the present study, we fabricated Al_2O_3-coated GaN nanowires by heating a mixture of GaN and Al powers.

To the best of our knowledge, this is the first report on the preparation of GaN/Al_2O_3 core-shell nanowires via a one-step fabrication technique. In addition, we suggest a possible growth mechanism. In our attempt to prepare nanowires, we accidentally discovered a novel spontaneous phase separation within the Ga-N-Al-O alloy system. This approach will provide an inexpensive and simple scheme to support applications in future, ultra-large-scale integration devices and nanosystems.

Experimental

We synthesized GaN/Al_2O_3 core-shell nanostructures in a 51 mm inner-diameter quartz tube by means of directly heating a mixture of GaN and Al powders (volume ratio = 1 : 1). An alumina boat holding both the substrate and the mixed powders was placed inside a quartz tube in a horizontal tube furnace. The substrate was kept at the preset reaction temperature for 1 h under a constant flow of NH_3 (flow rate: 20 sccm) and Ar (flow rate: 100 sccm). The synthesis temperature was optimized in the preliminary experiments and was set at 900 °C. An Au layer (about 3 nm) on the Si substrate was deposited by ion sputtering (Emitech, K757X).

The as-synthesized product was examined by X-ray diffraction (XRD, Philips X'pert MRD diffractometer), scanning electron microscopy (SEM, Hitachi S-4300 SE), transmission electron microscopy (TEM), selected area diffraction (SAD), and energy-dispersive X-ray spectroscopy (EDX, attached to TEM). PL spectroscopy was conducted at room temperature with the 325 nm line from a He-Cd laser (Kimon, 1K, Japan) at KBSI.

Results and Discussion

Fig. 1(a) shows a top-view SEM image of the product at a growth temperature of 900 °C. Based on the

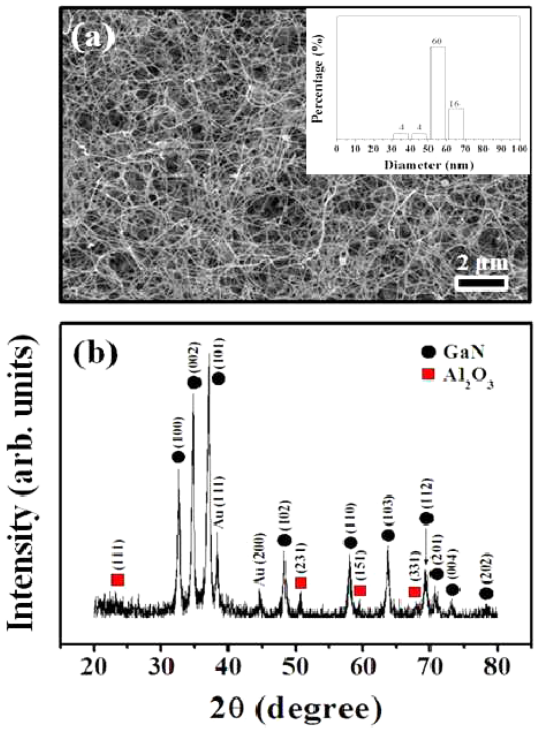

Fig. 1. (a) Top-view SEM image (Upper-right inset: diameter distribution) and (b) XRD pattern of the as-synthesized nanowires.

diameter distribution graph (in upper-right inset of Fig. 1(a)), we have calculated the average diameters of the 1D nanostructures. The average diameters of the nanowires are about 46.6 nm. Fig. 1b shows an XRD pattern. Apart from the peaks of the cubic Au phase with lattice parameter of a = 4.0786 Å (JCPDS File No. 04-0784), which originated from the substrate, the most recognizable reflection peaks could be indexed to the diffraction peak in regard to the hexagonal GaN phase with a lattice parameter of a = 3.186 Å and c = 5.178 Å (JCPDS File No. 02-1078). In addition, there exist relatively weak diffraction peaks in regard to the orthorhombic Al_2O_3 phase with a lattice parameter of a = 4.844 Å, b = 8.330 Å and c = 8.955 Å (JCPDS File No.88-0107).

Fig. 2(a) shows a low-magnification TEM image of a nanowire, indicating not only that the core structure has a straight-line morphology, but also that the outer solid layer is relatively smooth and continuous along the nanowire. From Fig. 2(a), the diameter of the core structure and the average thickness of each shell layer were measured at 22 nm and 4.5 nm, respectively. On the other hand, the arrowhead in the upper-left corner of the figure indicates that the tip part of the nanowire does not comprise the metallic nanoparticle. Figs. 2(b) and 2(c) show the EDX line profiles of Ga and Al, respectively, across the diameter of a coaxial nanowire, confirming the existence of elemental Ga with a rather uniform intensity profile; there is a valley-like profile for Al. With the XRD data (Fig. 1(b)) revealing the

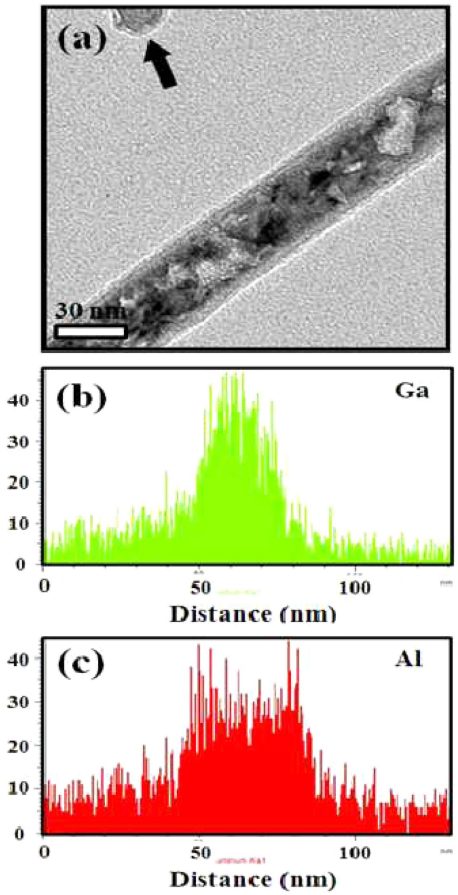

Fig. 2. (a) TEM image of a core-shell nanowire. The arrowhead indicates a tip part of a core-shell nanowire. (b, c) EDX line profiles of (b) Ga and (c) Al, respectively, across the GaN/Al_2O_3 core-shell nanowire.

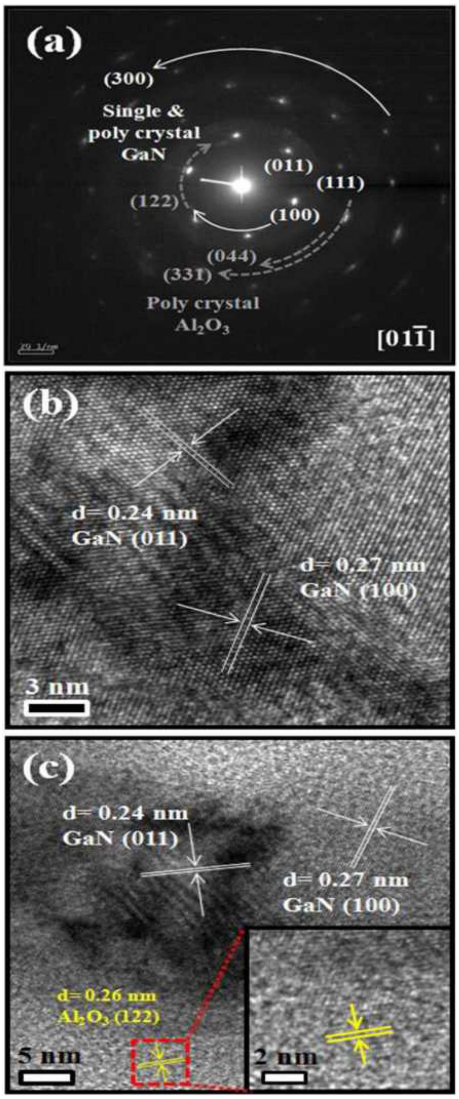

Fig. 3. (a) SAD pattern and (b,c) corresponding lattice-resolved TEM images taken from (b) the center and (c) the surface region of the core-shell nanowire in Fig. 2a.

presence of GaN and Al_2O_3 phases, EDX line profiles and the TEM image are in good agreement with the predicted profiles for the Al_2O_3-shelled GaN nanowires.

For a detailed investigation, the lattice-resolved TEM image and SAD pattern were examined. Fig. 3(a) shows the SAD pattern taken from the square box in Fig. 2(a); this was recorded perpendicular to the rod axis, as it was indexed for the [01$\bar{1}$] zone axis of crystalline hexagonal GaN. The pattern corresponds to a complicated structure, but a closer examination reveals that it consists of ring spots corresponding to poly-crystalline/single-crystalline hexagonal GaN. The single-crystal diffraction spots were indexed as the hexagonal GaN, including (011) and (111) reflections, etc. The poly-crystalline diffraction rings were indexed as the hexagonal GaN, including (100) and (300) reflections, etc. In addition, the SAD pattern shows the presence of weaker ring patterns, presumably corresponding to the polycrystalline structures of orthorhombic Al_2O_3 ((122), (044), and (331) reflections). Fig. 3b shows a lattice-resolved TEM image, enlarging an area near the center of the nanowire in Fig. 2(a). In spite of the shell coating, lattice fringes are clearly visible in the GaN core region. The interplanar spacings between the two neighboring fringes are about 0.24 nm and 0.27 nm, agreeing with the interplanar distance of the (011) and (100) planes of the hexagonal GaN lattice. Although some part of the shell layer was found by TEM observation to be crystalline orthorhombic Al_2O_3 (Fig. 3(c)), TEM investigation does not clearly show the lattice fringes of the Al_2O_3. Accordingly, we suppose that the sheath layer must be amorphous and/or polycrystalline.

Based on the above observations, we speculated on the growth mechanism of the core-shell nanowires. Up to the present, a lot of of 1D core-shell nanostructures have been synthesized, and there are two well-accepted mechanisms: the vapor-solid-liquid (VLS) and the vapor-solid (VS) mechanisms. From the TEM observation, no Au particles are clearly observed at the ends of the nanowires. Accordingly, it is not possible to regard the main growth mechanism as the Au-catalyzed tip-

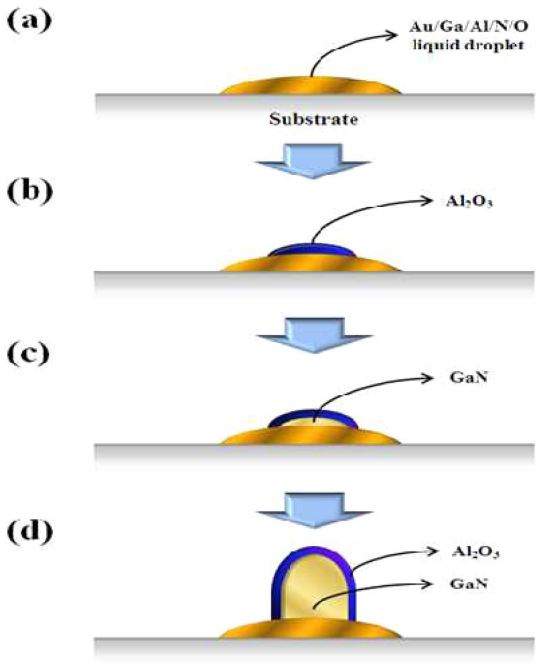

Fig. 4. Schematic illustration of a possible growth mechanism: (a) The initial stage, in which the liquid droplet is formed, (b) the middle stage, in which solid Al_2O_3 becomes precipitated, (c) the middle stage, in which solid GaN becomes precipitated underneath the predeposited Al_2O_3 shell, and (d) the final stage, in which the GaN/Al_2O_3core-shell nanowire is continuously grown.

growth VLS process. Some previous studies have reported the fabrication of core-shell nanowires via a VS route. In the typical VS-typed process, core nanowires from one source are first generated and, subsequently, the vapors from the other source are directly adsorbed onto the cores. For example, in the growth of SiC/Al_2O_3 core-shell nanowires, the Si in the SiC core has been found to originate from the Si substrate [54]. The formed Al_2O_3 cluster will diffuse to the upstream Si substrate and adsorb onto the surface of the SiC nanowires. In the fabrication of SiC/BN core-shell nanowires, the BN shell was found to originate from the BN crucible [55]. The BN layers from the BN crucibles were deposited on the outer surfaces of the SiC nanocable nucleus, forming SiC/Al_2O_3 core-shell nanowires. However, in the present case, both core and shell structures are thought to originate from the same source, which is a mixture of powders. Accordingly, it is unlikely that the core-shell nanowires were formed via a sequential process in which the GaN stem nanowires formed first and were subsequently coated with Al_2O_3 shell layers. Also, TEM investigation indicated that the shell thickness did not significantly vary along the wire length for any given nanowire (Fig. 2(a)). If the Al_2O_3 shell layer was formed via the direct adsorption of gas species during the growth of GaN nanowires, the nanowire diameter should vary from the bottom to the tip. Instead, we surmise that the growth proceeded by the diffusion through the alloy particles to form the core nanowire and the migration of Al_2O_3 on the surface of the alloy particle to the nanowire interface in a simultaneous growth process. Similarly, Moore et al. proposed a growth model for ZnS/SiO core-shell nanowires, in which the ZnS core was formed by volume diffusion across the catalyst particles while the silica shell was formed by surface diffusion on the catalyst particle [56].

In the present case, we suggest that the alloy particle/clusters reside at the bottom of the nanowires, which is called a base-growth mechanism, and which can be included in the VLS-typed process. Similarly, previous studies on the production of carbon nanotubes [57], MgO nanowires [58], and GeO_2 nanostructures [59] have revealed that such growth could be ascribed to a base growth mechanism, wherein the metal catalyst remains situated at the bottom of the nanostructures.

Herein, we illustrate a possible growth model for GaN/Al_2O_3 core-shell structures (Fig. 4). In the first step, a mixture of GaN and Al powders was heated and evaporated, forming Au/Ga/Al/N/O liquid droplets on the substrate with the incorporation of Ga, Al, N and O vapor species from the ambient (Fig. 4(a)). There are several oxygen sources in the present experiments, including residual oxygen in the chamber, leakage of the low vacuum system, and native oxide oxygen on the wafer surface. We surmise that the GaN powder will evaporate to be dissociated into Ga and N_2 vapors. In a previous study, GaN nanowires were grown via the following reaction: $Ga + NH_3 \rightarrow GaN + 3/2H_2$ [60]. The Al powders can be evaporated to become Al vapors. In this case, the growth temperature should have exceeded the eutectic temperature. The main candidates of compounds should be GaN, AlN, Ga_2O_3, and Al_2O_3. The free energies of formation (ΔG_f) at the growth temperature of 900 °C for GaN, AlN, Ga_2O_3, and Al_2O_3, are about -176, -371, -1269, and -1812 kJ/mol, respectively. From the thermodynamic considerations, the Al_2O_3 compound will preferentially form in the first place, with the Ga and N atoms remaining in the droplets. The remaining Ga and N atoms will subsequently form the GaN compound. However, it is not clear when and how the Al_2O_3 outer shell is formed. One possibility is that the Al vapor is barely soluble in the liquid droplet for some unknown reason. The Al vapor can be oxidized in the course of the surface diffusion process, ultimately forming the solid Al_2O_3 shell. The other possibility is that the relatively low density of the Al_2O_3 compound plays a crucial role. The densities of GaN and Al_2O_3 compounds are 6.15 and 3.95 g/cm^3, respectively. Accordingly, it is expected that the generated Al_2O_3 compound will float on the surface of the liquid droplet, with the GaN compound remaining inside the droplet (Fig. 4(b)). Subsequently, the liquid droplet will soon be supersaturated with GaN, and the solid GaN will nucleate underneath the

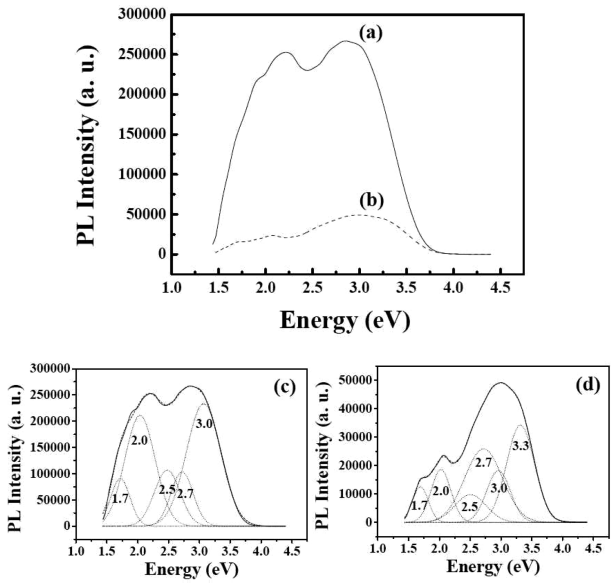

Fig. 5. Room temperature PL spectra of (a) GaN nanowires and (b) Al_2O_3-sheathed GaN nanowires. Gaussian fitting analyses of (c) core GaN nanowires and (d) Al_2O_3-sheathed GaN nanowires.

Al_2O_3 compound layer (Fig. 4(c)). The incorporation of Ga, N, Al, O gas species onto the bottom of the liquid droplet will continue, and the supersaturated Al_2O_3 will grow onto the predeposited Al_2O_3 outer layer. Similarly, the GaN will grow onto the pregenerated GaN nanostructure. Ultimately, GaN/Al_2O_3, core-shell nanowires will be formed, as depicted in Fig. 4(d).

Figs. 5(a) and 5(b) show the PL emission spectra of the uncoated and Al_2O_3-sheathed GaN nanowires, respectively. Multi-peak Gaussian fitting analysis reveals that the PL spectrum of the uncoated GaN nanowires mainly consists of five bands, which peak at approximately 1.7, 2.0, 2.5, 2.7, and 3.0 eV (Fig. 3(c)). On the other hand, the PL spectrum of the Al_2O_3-sheathed GaN nanowires mainly consists of six bands, which peak at approximately 1.7, 2.0, 2.5, 2.7, 3.0, and 3.3 eV (Fig. 3(d)). In order to reveal the origin of bands, we have compared PL spectrum of the Al_2O_3-sheathed GaN nanowires with that of the pure GaN nanowires. It can be seen that the overall intensity has been significantly reduced by adding a shell layer (Figs. 5(a) and 5(b)). Since GaN is a highly luminescent material, the Al_2O_3 shell layer has significantly reduced the amount of emission from the GaN core by means of the shielding effect. The blue emission (2.7 eV) in GaN is ascribed to crystal defects such as V_{Ga}-related complexes [61-63], whereas the violet emission (3.0 eV) is ascribed to various defects in GaN, including dislocations and vacancies [64]. Both yellow (2.0 eV) and green (2.5 eV) emissions in GaN are known to be related to structural defects [65-67]. In particular, the red emission band (1.7 eV) of GaN originates from a donor-acceptor pair (DAP) transition process involving the deep acceptor $V_{Ga}O_N$ [68,69]. Also, it is noteworthy that a new peak around 3.2 eV has been added by the Al_2O_3-coating. It has been known that F^+ (oxygen vacancies with one electron) centers in Al_2O_3 cause UV bands centered around 3.2 eV [70, 71]. Previously, near-band-edge emission in ZnO nanorod arrays was considerably enhanced by the presence of Al_2O_3 shells [72].

Conclusion

By means of a one-step evaporation technique, novel GaN/amorphous Al_2O_3 core-shell 1D structures were synthesized by the simple heating of a mixture of GaN and Al powders. The produced nanostructures typically consisted of a core of single crystalline GaN nanowires and a shell of Al_2O_3 tubular structures. Owing to the absence of Au-related nanoparticles at the tip, we propose as the dominant mechanism for the growth of the core/shell nanowires a base-growth mechanism. Also, we discussed a possible growth mechanism, explaining the preferential formation of the Al_2O_3 shells on the outside of the core-shell nanowires. In terms of Gaussian convolution analysis, room-temperature PL measurements of the core/shell nanowires exhibit six emission bands. Among these, the bands at 1.7, 2.0, 2.5, 2.7, and 3.0 eV are attributed to the GaN core, whereas the band at 3.3 eV is attributed to the Al_2O_3 shell. The Al_2O_3 sheaths will provide perfect electrical isolation of the GaN cores, proposing the application of the prepared nanowires in nano-electronic devices.

Acknowledgments

This research as supported by Basic Science Research Program through the National Research Foundation of Korea (NRF) funded by the Ministry of Education, Science and Technology (2011-0009946).

References

1. J. Zolper, R. Shul, A. Baca, R. Wilson, S. Pearton and R. Stall, Appl. Phys. Lett. 68 (1996) 2273.
2. B. Liu, Y. Bando, C. Tang, F. Xu, J. Hu and D. Golberg, J. Phys. Chem. B 109 (2005) 17082.
3. M. Lee, F. Xia, W.T. Nichols, C, Choi and W.I. Park, Met. Mater. Int. 18 (2012) 875.
4. B. Lee, J.H. Seo, J.P. Ahn, H. Kwon and H.R. Yang, Met. Mater. Int. 18 (2012) 727.
5. S. Kim, M.S. Kim, G. Nam and J.-Y. Leem, Electron. Mater. Lett. 8 (2012) 445.
6. H.W. Kim, J.C. Yang, H.G. Na and D.S. Kwak, C. Lee, Met. Mater. Int. 18 (2012) 705.
7. M.-Y. Kim, B.-K. Yu and T.-S. Oh, Electron. Mater. Lett. 8 (2012) 269.
8. M.-S. Seo and H. Lee, Electron. Mater. Lett. 8 (2012) 259.
9. S.-H. Lee and G.-H. Jeong, Electron. Mater. Lett. 8 (2012) 5.
10. J.S. Han, C. Lee and J. Lee, Electron. Mater. Lett. 8 (2012) 21.
11. B. Kim and B.-K. Park, Electron. Mater. Lett. 8 (2012) 33.
12. S.-S. Chee and J.-H. Lee, Electron. Mater. Lett. 8 (2012) 53.

13. S. Kim, J.-W. Jung, T.-S. Lee, S.-M. Yang and J.-R. Jeong, Electron. Mater. Lett. 8 (2012) 71.
14. Y. Oh, S. Nam, S. Wi, S. Hong and B. Park, Electron. Mater. Lett. 8 (2012) 91.
15. M. Martyniuk, G. Parish, H. Marchand, P.T. Fini, S.P. DenBaars and L. Faraone, Electron. Mater. Lett. 8 (2012) 111.
16. W. Czubatyj and S.J. Hudgens, Electron. Mater. Lett. 8 (2012) 157.
17. J. Kim, M. Eom, S. Noh and D. Shin, Electron. Mater. Lett. 8 (2012) 209.
18. T. Prakash, Electron. Mater. Lett. 8 (2012) 231.
19. Y. Chen, S.Y. Yang and J. Kim, Electron. Mater. Lett. 8 (2012) 301.
20. S.-S. Chee and J.-H. Lee, Electron. Mater. Lett. 8 (2012) 315.
21. A. Tarale, Y.D. Kolekar, V.L. Mathe, S.B. Kulkarni, V.R. Reddy and P. Joshi, Electron. Mater. Lett. 8 (2012) 381.
22. L. Guo, W.Y. Yoon and B.K. Kim, Electron. Mater. Lett. 8 (2012) 405.
23. P.L. Gong and H. Li, Electron. Mater. Lett. 8 (2012) 471.
24. C. Liu, Z. Liu, L.E, Y. Li, J. Han, Y. Wang, Z. Liu, J. Ya, and X. Chen, Electron. Mater. Lett. 8 (2012) 481.
25. S.H. Lee, H.J. Lee, H. Shiku, T. Yao and T. Matsue, Electron. Mater. Lett. 8 (2012) 511.
26. J. Park and K. Kim, Electron. Mater. Lett. 8 (2012) 545.
27. P.A. Chate, S.S. Patil, J.S. Patil, D.J. Sathe and P.P. Hankare, Electron. Mater. Lett. 8 (2012) 553-558.
28. W.-G. Lee, E. Kim and J. Jung, Electron. Mater. Lett. 8 (2012) 609.
29. B. Ha, S.H. Seo, J.H. Cho, C.S. Yoon, J. Yoo, G.C. Yi, C.Y. Park and C.J. Lee, J. Phys. Chem. B 109 (2005) 11095.
30. B.D. Liu, Y. Bando, C.C. Tang, F.F. Hu, J.Q. Hu and D. Golberg, J. Phys. Chem. B 109 (2005) 17082.
31. X.M. Cai, A.B. Djurišiæ and M.H. Xie, Thin Solid Films 515 (2006) 984.
32. H.M. Kim, Y.H. Choo, H. Lee, S.I. Kim, S.R. Ryu, D.Y. Kim, T.W. Kang and K.S. Chung, Nano Lett. 4 (2004) 1059.
33. Y. Huang, X. Duan, Y. Cui and C.M. Lieber, Nano Lett. 2 (2002) 101.
34. Y.B. Li, Y. Bando, D. Golberg and Y. Uemura, Appl. Phys. Lett. 83 (2003) 3999.
35. L.J. Lauhon, M.S. Gudiksen, C.L. Wang and C.M. Lieber, Nature 420 (2002) 57.
36. Y. Zhang, K. Suenage, C. Colliex and S. Iijima, Science 281 (1998) 973.
37. Y.B. Li, Y. Bando, D. Golberg and Y. Uemura, Appl. Phys. Lett. 83 (2003) 3999.
38. Y. Wang, Z. Tang, X. Liang, L.M. Liz-Marzan and N.A. Kotov, Nano Lett. 4 (2004) 225.
39. X. Liang, S. Tan, Z. Tang and N.A. Kotov, Langmuir 20 (2004) 1016.
40. C.-C. Tang, X.-W. Xu, L. Hu and Y.-X. Li, Appl. Phys. Lett. 94 (2009) 243105.
41. J.W. Chung, O.I. Saadat, J.M. Tirado, X. Gao, S. Gao and T. Palacios, IEEE Electron. Device Lett. 30 (2009) 904.
42. L.J. Lauhon, M.S. Gudiksen, D. Wang and C.M. Lieber, Nature 420 (2002) 57.
43. Y.C. Chang, W.H. Chang, H.C. Chiu, L.T. Tung, C.H. Lee, K.H. Shiu, M. Hong, J. Kwo, J.M. Hong and C.C. Tsai, Appl. Phys. Lett. 93 (2008) 053504.
44. Y. Wang, Y. Li, K. Yu and Z. Zhu, J. Phys. D: Appl. Phys. 44 (2011) 105301.
45. C.Y. Chen, C.A. Lin, M.J. Chen, G.R. Lin and J.H. He, Nanotechnology 20 (2009) 185605.
46. C.-C. Wang, C.-C. Kei, Y. Tao and T.-P. Perng, Electrochem. Sol. Stat. Lett. 12 (2009) K49.
47. D.-Y. Chen, M.-W. Shao, L. Cheng, X.-H. Wang and D. D.-D. Ma, Appl. Phys. Lett. 94 (2009) 043101.
48. C. Li, X. Wang, G. Chen, L. He and H. Cao, Chem. Lett. 39 (2010) 64.
49. Y. Li, Y. Li, J. Tang, H. Lin, N. Yao, X. Shen and C. Deng, J. Chromatography A 1172 (2007) 57.
50. W. Liu, W. Zhong, H.Y. Jiang, N.J. Tang, X.L. Wu and W.Y. Du, Eur. Phys. J. B 46 (2005) 471.
51. H.-P. Peng, R.-P. Liang and J.-D. Qiu, Biosens. Bioelectron. 26 (2011) 3005.
52. M. Law, L.E. Greene, A. Radenovic, T. Kuykendall, J. Liphardt and P. Yang, J. Phys. Chem. B 110 (2006) 22652.
53. M. Kang, J.S. Lee, S.K. Sim, B. Min, K. Cho, H. Kim, M.Y. Sung, S. Kim and M.S. Lee, Thin Solid Films 466 (2004) 265.
54. H. Cui, L. Gong, Y. Sun, G. Z. Yang, C.L. Liang, J. Chen and C.X. Wang, Cryst. Eng. Comm. 13 (2011) 1416.
55. Y. Li, P.S. Dorozhkin, Y. Bando and D. Golberg, Adv. Mater. 17 (2005) 541.
56. D. Moore, J.R. Morber, R.L. Snyder and Z.L. Wang, J. Phys. Chem. B 112 (2008) 2895.
57. S. Fan, M.G. Chapline, N.R. Franklin, T.W. Tombler, A.M. Cassell and H. Dai, Science 283 (1999) 512.
58. H.W. Kim and S.H. Shim, Chem. Phys. Lett. 422 (2006) 165.
59. H.W. Kim and J.W. Lee, Physica E 40 (2008) 2499.
60. J. Li, C. Lu, B. Maynor, S. Huang and J. Liu, Chem. Mater. 16 (2004) 1633.
61. M.A. Reshchikov and H. Morkoc, J. Appl. Phys. 97 (2005) 61301.
62. M.A. Reshchikov and R.Y. Korotkov, Phys. Rev. B 64 (2001) 115205.
63. H.C. Yang, T.Y. Lin and Y.F. Chen, Phys. Rev. B 62 (2000) 12593.
64. S.M. Lee, M.A. Belkhir, X.Y. Zhu, Y.H. Lee and Y.G. Hwang, T. Frauenheim, Phys. Rev. B 61 (2000) 16033.
65. M.A. Reshchikov, H. Morkoc, S.S. Park and K.Y. Lee, Appl. Phys Lett. 78 (2001) 3041.
66. A. Castaldini, A. Cavallini and L. Polenta, Appl. Phys. Lett. 87 (2005) 22105.
67. T. Suski, P. Perlin, H. Teisseyre, M. Leszczynski, I. Grzegory, J. Jun, M. Bockowski, S. Porowski and T. D. Moustakas, Appl. Phys. Lett. 67 (1995) 2188.
68. L. Wang, E. Richter and M. Weyers, Phys. Stat. Sol. (a) 204 (2007) 846.
69. S. Zeng, G.N. Aliev, D. Wolverson, J.J. Davies, S.J. Bingham, D.A. Abdulmalik, P.G. Coleman, T. Wang and P.J. Parbrook, Phys. Stat. Sol. (c) 3 (2006) 1919.
70. X.S. Peng, L.D. Zhang, G.W. Meng, X.F. Wang, Y.W. Wang, C.Z. Wang and G.S. Wu, J. Phys. Chem. B 106 (2002) 11163.
71. B.D. Evans and M. Stapelbroek, Phys. Rev. B (1978) 7089.
72. C.Y. Chen, C.A. Lin, M.J. Chen, G.R. Lin and J.H. He, Nanotechnology 20 (2009) 185605.